Reconfigurations within resonating communities of brain regions following TMS reveal different scales of processing

Javier O. Garcia*[1,2], Arian Ashourvan[1,2], Steven M. Thurman[1], Ramesh Srinivasan[4,5], Danielle S. Bassett[2,3], Jean M. Vettel[1,2,6]

[1]U.S. Army Research Laboratory, Aberdeen Proving Ground, MD
[2]Department of Bioengineering, University of Pennsylvania, Philadelphia, PA
[3]Department of Electrical & Systems Engineering, University of Pennsylvania, Philadelphia, PA
[4]Department of Cognitive Sciences, University of California, Irvine, Irvine, CA
[5]Department of Biomedical Engineering, University of California, Irvine, Irvine, CA
[6]Psychological and Brain Sciences, University of California, Santa Barbara, Santa Barbara, CA

Running Head: Network reconfigurations following TMS

Keywords: neuroimaging, network flexibility, network allegiance, local-global processing, TMS, EEG

***Corresponding Author:**
Javier Omar Garcia
E: javier.o.garcia.civ@mail.mil
RDRL-HRS-C (ARL/HRED/TNB)
459 Mulberry Point Road
Aberdeen Proving Ground, MD 21005

ABSTRACT

An overarching goal of neuroscientific research is to understand how heterogeneous neuronal ensembles cohere into networks of coordinated activity to support perception, cognition, and adaptive behaviors. To investigate the interplay between local and global dynamics in the brain, we use a method from network science that identifies the modular hierarchical architecture of the brain, where modules (or sub-networks) perform segregated and highly specialized processing. In this study, we measured electroencephalography (EEG) while single pulses of transcranial magnetic stimulation (TMS) were applied to occipital and parietal cortices to measure rapid network reconfigurations within specific frequency bands of the EEG signals. We compute functional connectivity between pairs of estimated brain sources, and we examine dynamic network communities by characterizing two distinct features of network reconfiguration, *flexibility* and *allegiance*, among spatially distributed neural sources following TMS stimulation. Using distance from the stimulation site to infer local and global effects, we find that alpha activity (8-12Hz) reflects concurrent local and global effects on network dynamics. Pair-wise allegiance of brain regions to communities on average increased near the stimulation site, whereas TMS-induced changes to flexibility were generally invariant to distance and stimulation site. In contrast, communities within the beta (13-20Hz) band demonstrated a high level of spatial specificity, particularly within a cluster comprising paracentral areas. Together, these results suggest that focal magnetic neurostimulation to distinct cortical sites can help identify both local and global effects on brain network dynamics, and highlight fundamental differences in the manifestation of network reconfigurations within alpha and beta frequency bands.

NEW & NOTEWORTHY

TMS may be used to probe the causal link between local regional activity and global brain dynamics. Using simultaneous TMS-EEG and dynamic community detection, we introduce what we call “resonating communities”, or frequency band-specific communities in the brain, as a way to index local and global processing. These resonating communities within the alpha and beta bands brain display both global (or integrating) behavior and local specificity, highlighting fundamental differences in the manifestation of network reconfigurations.

INTRODUCTION

The brain is an intricate collection of heterogeneous areas (Alivisatos et al., 2012), and a central goal of neuroscientific research is to understand how the coordination of these different regions support cognition (Azevedo et al., 2009; Bressler and Menon, 2010; Gollo et al., 2017). One theoretical approach encapsulates the coordinated activity into a framework of scales, and research has examined how local regional activity harmonizes with global signals (Bressler and Kelso, 2001). *Local activity* refers to cortical or thalamocortical interactions and reflects the transient coordination of inhibitory and excitatory neighboring neurons, constrained by basic neurophysiological factors such as refractory limitations and synaptic rising (Fries et al., 2007). However, research has shown that this local neural activity can be modulated by global activity in the brain (for review, see Buzsáki and Draguhn, 2004; Buzsáki and Wang, 2012). *Global activity* arises from propagation delays in cortico-cortical fibers and reflects the dynamic interactions and synchronization among distal networks. This conceptual framework of local and global networks interacting in cognitive processes is critical to the interpretation of neurophysiological signals. Yet, how this activity coheres to manifest cognition is still an active area of study (Bressler and Kelso, 2001; Cocchi et al., 2017).

EEG affords a natural way to study both local and global processing by examining oscillatory dynamics in different frequency bands (Buzsáki and Draguhn, 2004; Canolty and Knight, 2010). Changes in power in high frequencies, such as beta and gamma, have been used to infer local dynamics arising from the synchronization of populations of neurons (Brunel and Wang, 2003; Geisler et al., 2005). Similarly, the emergent activity in slower EEG frequencies, ranging across delta, theta, and alpha, has been interpreted as global activity arising from long-distance coordination of synchronized neural firing in disparate brain regions (Brunel and Wang, 2003; Geisler et al., 2005). Collectively, results from EEG studies have indicated the importance of both local and global activity, indexed by high- and low-frequency oscillations, for understanding variability in human behavior (Buzsaki, 2006; Nunez and Srinivasan, 2006; Nunez et al., 2001; Volberg et al., 2009). However, EEG provides only an inferential

framework to study interactions between local and global activity. Advancements in neurostimulation paradigms provide an avenue to directly study the causal role of local changes in oscillatory dynamics (Bergmann et al., 2016; Pascual-Leone et al., 2000).

Transcranial magnetic stimulation (TMS) has been proposed as a method to probe the dynamic interplay between local processing and the consequent global interactions with more distal regions of the brain (Massimini et al., 2009; Romei et al., 2012). Traditionally, single pulse TMS is a technique used to induce a short controlled burst of activity in a predetermined local brain region, directly causing a change in the local dynamics (Pascual-Leone et al., 2000). Research has identified behavioral outcomes from local stimulation for patients in clinical settings and healthy individuals in experimental tasks. Local stimulation in patients can successfully determine stroke recovery (for review, Auriat et al., 2015), mitigate severe affective disorders (e.g., Berman et al., 2000), and preserve motor and language functions in presurgical mapping (Eldaief et al., 2013). TMS has also been successfully employed to confirm the role of an individual brain region on task performance, ranging from sensory attention (Herring et al., 2015; Romei et al., 2013; Taylor and Thut, 2012) to working memory performance (Brunoni and Vanderhasselt, 2014; Rose et al., 2016). More recently, experimental research has suggested that the brain alterations caused by TMS is not limited to local perturbations (Sale et al., 2015). By pairing TMS with other imaging modalities, it provides an innovative approach to study connectivity relationships among disparate brain regions (Cocchi et al., 2015; Mancini et al., 2017; Siebner et al., 2009).

Multimodal studies have paired TMS with functional neuroimaging, such as fMRI (e.g., Bestmann et al., 2008; Bohning et al., 1999), EEG (e.g., Bortoletto et al., 2015; Garcia et al., 2011), and PET (e.g., Paus, 1998), and measured stimulation-induced responses in brain areas that are distal to the stimulation site, indicating that stimulation can induce transient coordination between local and global activity (Bestmann et al., 2008; Driver et al., 2009; Paus, 1998). Complementing these findings, computational models of neurodynamics has demonstrated that regional differences in structural

connectivity may account for how local network activity that is induced from a focal TMS pulse propagates along cortico-cortical fibers to influence global network synchronization (Gollo et al., 2017; Muldoon et al., 2016). While both experimental and modeling work has suggested the importance of interacting networks, few studies have employed the rich set of tools of network science to understand the propagation of stimulation (Bortoletto et al., 2015). Network science not only provides a mathematical language to describe complex connectivity patterns resulting from stimulation, but previous research has also proposed a variety of summary metrics in which to characterize local and global connectivity in the brain (for review, see Garcia et al., 2018). In this study, we address this existing gap in the literature and employ a method recently developed in network science to study the interactions of local connectivity and global network dynamics.

We investigated network reconfigurations from resting state EEG following single pulses of transcranial magnetic stimulation (TMS) using a method from network science that reveals modular architecture in the brain (Bassett and Bullmore, 2006; Bullmore and Sporns, 2012; Ercsey-Ravasz et al., 2013). Participants received single pulses of TMS to occipital or parietal cortex, and we computed functional connectivity using EEG data for a two second epoch surrounding stimulation (-1 to 1). Our theoretical question focused on the comparison between stimulation to spatially-disparate, large lobes of the brain, investigating how stimulation influenced network dynamics following stimulation as indexed by the modular architecture of the functional connectivity patterns. Each module is composed of regions with synchronized activity that are thought to be dynamically linked for the purpose of cohesive processing (Achard et al., 2006; Bassett and Bullmore, 2006; Sporns et al., 2004). To index local and global activity, we investigate two frequency bands that probe brain dynamics across these scales. We separately characterize the modular architecture of resting-state EEG within the alpha band and within the beta band, from which we define *resonating communities,* or communities of brain regions restricted to a specific frequency band. This delineation was inspired by the theoretical proposal by Rosanova and colleagues (2009) that posits brain regions have primary resonant frequencies: resting state activity is

dominated by alpha in the occipital cortex, while parietal activity is dominated by beta activity. Consequently, our analysis investigates whether network changes in these frequency bands differentiate the location of the stimulation.

Changes in functional network organization before and after stimulation were characterized using two metrics: *module allegiance* and *network flexibility.* Allegiance estimates how often regions communicate with subnetworks in the community structure and demonstrate the same pattern of connectivity across time points. Flexibility, by contrast, reveals the extent to which a region remains a member of the same module over time, or whether it frequently (and flexibly) changes its assignment across modules between time points. These two metrics are uniquely suited to investigate local and global processing following stimulation since they capture both the general shifts in communities across time for any individual node (local) and the unique shifts between each pair (global). Unlike other metrics that investigate the temporal dynamics of network connectivity (for review, see Garcia et al., 2018), allegiance and flexibility capture the extreme cases dynamics changes in local and global connectivity. Using these measures, we report substantial differences between the alpha and beta band communities. While the alpha network reveals a dynamic interplay of local and global connectivity, communities within the beta band display a spatial specificity across both metrics, which suggest a more *local* connectivity impact of stimulation. Together, these results show that focal TMS to distinct cortical sites can help identify both local and global effects on dynamic network configurations, and demonstrate fundamental differences in the manifestation of network effects in alpha and beta frequency bands.

METHODS & MATERIALS

Participants

Ten individuals (7 men, 3 women, aged 20-33, M = 23.8, STD = 4.8) participated in the TMS-EEG experiment. All gave informed, written consent as approved by the University of California, Irvine

Institutional Review Board.

TMS/EEG Data Collection

Data collection occurred in the TMS/EEG Laboratory in the Human Neuroscience Lab at the University of California, Irvine. The subjects were seated in a comfortable chair approximately 60 cm from the monitor, and their heads were fixed in a chinrest to minimize movement while they continuously fixated on the center of the monitor screen. No overt motor responses were required during the 30 min experimental session.

Stimulation was applied with a MagStim Model 200 Monophasic Stimulator P/N 3010-00 equipped with a figure-of-eight coil at 55% stimulator intensity (E-field 297 V/m), following the stimulation procedure developed in previous research (Garcia et al., 2011). This study targeted four regions that included symmetric areas in occipital and parietal cortices (Figure 1), and the location for these regions were estimated by electrodes O1/O2 and P1/P2 of the 10-20 international scheme for EEG. This method reliably targets a similar area across participants within 2cm of sulcal/gyral landmarks (Herwig et al., 2003), the resolution of high-density EEG used in this study. For occipital stimulation, the coil was oriented parallel to the coronal view (i.e., paddle pointed up), and for parietal stimulation, the coil was oriented at approximately tangential to the curvature of the scalp at the electrode target locations. For each region, participants completed a 7 min block of approximately 100 single pulses of stimulation that were no closer than 4 sec apart, following standard safety procedures (Rossi et al., 2009). Within a session, the 10 blocks were semi-randomly selected among the four stimulation sites (O1, O2, P1, P2), ensuring that multiple blocks of each stimulation type occurred in each session. Participants completed 4 sessions on separate days, providing an aggregate of 4000 total stimulation trials for each subject.

Throughout the session, 128 channels of EEG were recorded using a TMS-compatible EEG system from Advanced Neuro Technology (ANT, The Netherlands). The Waveguard cap system consisted of small Ag/AgCl electrode elements, specially designed to yield high-quality and stable

recordings with simultaneous TMS. EEG data were sampled at 1024 Hz for this experiment and impedances were targeted to be kept below 10 kΩ.

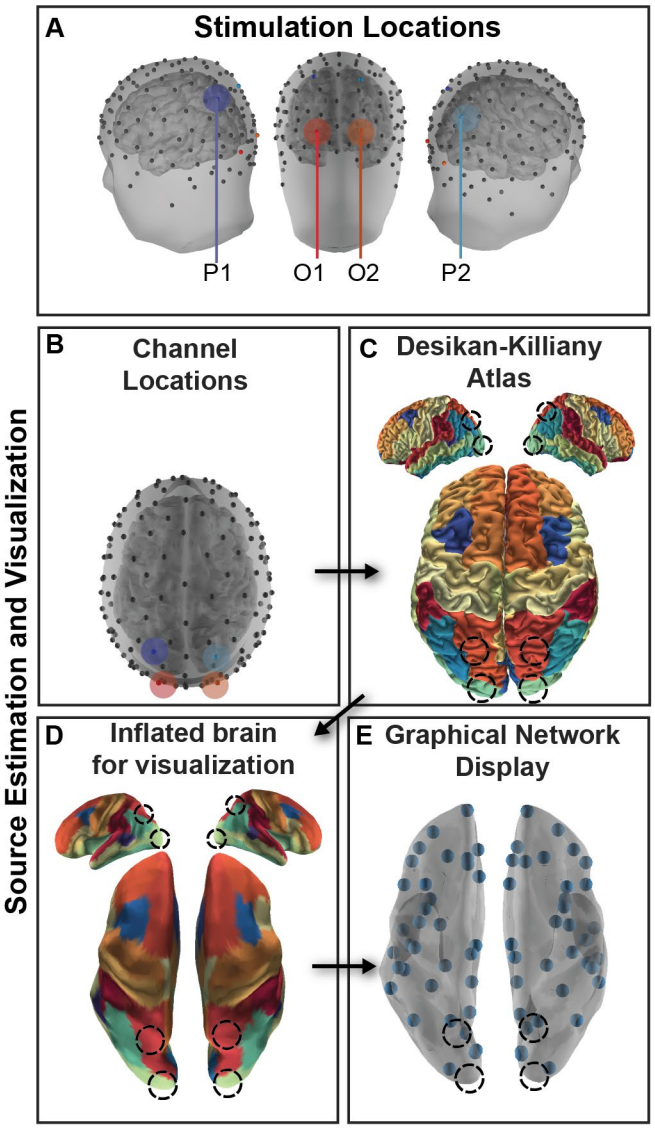

Figure 1: Experimental Design and Analysis. A. Participants received stimulation in symmetric regions in occipital (O1, O2) and parietal (P1, P2) cortex. B. High density EEG recorded from 128 channels was submitted to a cLORETA source analysis, and current source density (CSD) was estimated for each vertex of a high resolution mesh. C. CSD was then averaged within

a parcellation of cortex following the Desikan-Killiany atlas parcellation to estimate regional brain activity. D. The cortex was inflated for visualization. E. Each centroid of the region is plotted as a small orb. Stimulation locations marked in each visualization with a shaded region or a dotted line.

EEG Analysis

Segmentation of epochs

The EEG data were preprocessed following an established pipeline (Garcia et al., 2011) for each of the four sessions for each of the ten participants (40 total datasets). First, raw EEG were submitted to a principal component analysis (PCA) to identify the peak amplitude events that correspond to the stimulation event and to eliminate any timing discrepancy between the intended and actual timing of the stimulation pulse in the EEG data. After the timing of each pulse was recovered, the decomposition was discarded and was not used in any subsequent analysis (i.e., no components were removed). Using the maxima from the largest component of each dataset as the onset of stimulation, the 40 datasets were segmented into 40,000 epochs that were two seconds in duration, including one second (1024 samples) before and after the TMS pulse. After this segmentation procedure, each trial was normalized by the standard deviation of the 512 samples prior to the stimulation. Automated artifact editing based on amplitude thresholds was used to eliminate approximately 20% of trials likely contaminated with artifacts from the TMS pulse or blink artifacts. After this preliminary pre-processing, we largely followed the PREP approach, an artifact removal procedure that has been shown to be robust to artifacts within environments high artifact environments (Bigdely-Shamlo et al., 2015). The following steps were completed (1) line noise removal via a frequency-domain (multi-taper) regression technique to remove 60Hz and harmonics present in the signal, (2) a robust average reference with a Huber mean, (3) artifact subspace reconstruction to remove residual artifact with the standard deviation cutoff parameter was

set to 15, and (4) band-pass filtering using a Butterworth filter with 2-dB attenuation at 2 and 50 Hz.

Distributed Source Reconstruction

From the pre-processed EEG data, we estimated current source density (CSD) over a 5003-vertex cortical mesh. A boundary element method (BEM) forward model was derived from the 'Colin 27' anatomy (Holmes et al., 1998) and transformed into MNI305 space (Evans et al., 1993) using standard electrode positions fit to the Colin 27 head surface in BrainStorm (Tadel et al., 2011). The BEM solution was computed using OpenMEEG (Gramfort et al., 2010; Kybic et al., 2005), and the cLORETA approach was used for inverse modeling as described in detail in (Mullen et al., 2015) and implemented in the BCILAB (Kothe and Makeig, 2013) and Source Information Flow (Mullen, 2014) toolboxes. Finally, CSD was then averaged into one time course from each of the 68 regions of the Desikan-Killiany atlas (Desikan et al., 2006) and down sampled to 128Hz for use in the connectivity analysis.

Functional Connectivity Analysis

To estimate functional connectivity of brain networks before and after stimulation, an undirected measure, known as the debiased weighted phase lag index (dwPLI), was computed between each pair of the 68 estimated brain regions from the atlas. DwPLI is robust against the influence of volume conduction, uncorrelated noise, and intersubject variations in sample size (Vinck et al., 2011; Vindiola et al., 2014), and it has previously been proposed to be an appropriate pairing with a source localization analysis to minimize the influence of these nuisance variables (van Diessen et al., 2015; Hillebrand et al., 2012).

The connectivity estimates were calculated using Matlab and FieldTrip (Oostenveld et al., 2010). First, a multitaper spectral estimation was applied to the CSD measurements, and then dwPLI was computed between all source pairs to estimate the functional connectivity pattern of signals in the frequency range between 2Hz and 25Hz (step = 0.5 Hz) in a 2 sec window centered on the stimulation

pulse (-1sec to 1sec). The dwPLI connectivity estimates were calculated across trials, representing the trial-by-trial consistency between regional CSD for 51 non-overlapping 40msec time windows across the 2sec epoch. To determine overall connectivity increases or decreases across the brain, dwPLI estimates were normalized via a z-score transformation for each participant.

Dynamic Community Detection

In addition to looking at whole-brain connectivity patterns, we employed a community detection algorithm (Bassett and Bullmore, 2006; Bullmore and Sporns, 2012; Ercsey-Ravasz et al., 2013) to examine whether regions formed modular networks, and if the regional composition of these networks changed before and after stimulation across the 51 time windows in our 2 second epoch. The algorithm optimizes a multilayer modularity quality function, Q, using a Louvain-like greedy algorithm (Blondel et al., 2008; Mucha et al., 2010) to assign brain regions to communities. The community assignments are dependent on two parameters: (1) a structural resolution γ parameter and (2) a temporal resolution ω parameter. These two parameters determine the scale of the resulting graph, both structurally and temporally, and here, we sweep this parameter space to find the scale of the data that is most unlike that expected in an appropriate random network null model.

Following our previous work on fMRI data (Bassett et al., 2013), the values for both parameters were determined by comparing the mean value of *Q* in the experimental data to the mean value of Q in a shuffled null model of the data; we tested a range of values for each parameter since this algorithm has not yet been applied to EEG data, which has inherently different temporal and spatial scales of functional connectivity (Nunez and Srinivasan, 2006). Our analysis examined parameters for $\gamma = 0.8$ to $\gamma = 1.6$ and $\omega = 0.5$ to $\omega = 35$. The null model of the data was created by randomly shuffling the pair-wise dwPLI values, destroying the correlational structure observed in EEG data for each subject and parameter pairing. Each *Q* was then subtracted for each parameter pairing, comparing the observed model's *Q* (from the unperturbed EEG connectivity patterns) and the null model's Q_{null} (shuffled

connectivity patterns) for each subject. The largest difference was found for γ = 1.025 and ω = 9, and these parameters were used in the reported analyses. Since the community detection algorithm is non-deterministic (Good et al., 2010), 100 iterations of the hard partitions were estimated with modularity maximization for each subject and stimulation condition (O1, O2, P1, P2), yielding 100 sets of community labels for the 68 nodes for each of the 4 stimulation conditions for each of the 10 subjects.

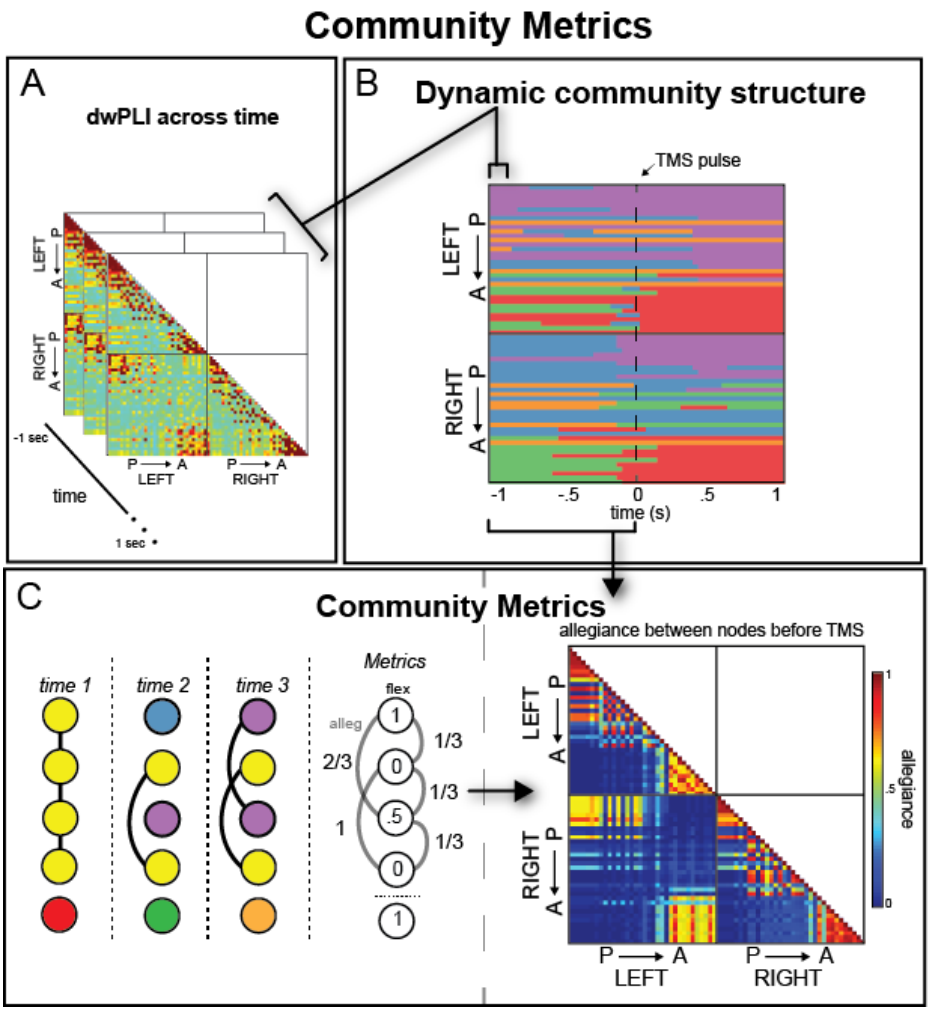

Figure 2: Overview of Analysis method and natural brain architecture. (A) DwPLI was estimated across trials in 40ms windows across the 2sec epoch, including one second before and one second after the TMS onset (P: posterior, A: anterior nodes). (B) Dynamic network communities from a sample subject derived from the dwPLI estimate for each window. Each color marks a different community label. (C, left) From B, community metrics were calculated that represent how often a node changes over

time (flexibility) or how often each node-pair is in the same community over time (allegiance). The cartoon networks show 5 hypothetical nodes that change communities over time (3 time windows shown). Connections are marked as black lines and metrics are given in the final column, showing a range of flexibility and allegiance values. These metrics are used in subsequent analyses. (C, right) Summary allegiance matrix for a sample subject for the period before TMS onset, indicating the natural architecture of connectivity within the alpha band.

Community Metrics

Within each of the 51 time windows of our 2 second stimulation epoch, we examined the relationship among the brain regions within a community to characterize the dynamic reconfiguration of spatially distributed neural sources before and after stimulation. Our analysis investigated two community metrics, allegiance (Bassett et al., 2015) and flexibility (Bassett et al., 2011). As illustrated in Figure 2, *allegiance* estimates how much regions communicate with subnetworks in the community structure and demonstrate the same pattern of connectivity across time points. Thus, allegiance increases the resolution of community and captures coordinated activity of each node with every other node in the brain. We also examined *flexibility*, which focuses on the connectivity of single brain regions, revealing whether a region remains a member of the same community over time or if it frequently (and flexibly) changes its assignment across communities throughout the experiment.

Each of these measures was calculated twice, once for the 25 windows of partitions before TMS (preTMS) and once for the 25 windows following TMS (postTMS), ignoring the center window where stimulation occurred. To calculate allegiance, each node's community label across the brain was compared for each time window and the number of times the both nodes in the pair were in the same community was counted. This value was then divided by the number of windows within the interval (25), and the allegiance values were averaged across the 25 windows separately for the preTMS and postTMS timeframes. Allegiance values were computed separately for each person, for 100 iterations, and then averaged across iterations and participants. Our analysis focused on the difference score

between preTMS and postTMS, which can be used to measure changes in dynamic community structure as a function of stimulation.

The same steps were used to examine differences in regional flexibility before and after stimulation, except that flexibility was computed by counting the number of times a single node changed communities, divided by the number of times a node could change communities (25).

Finally, results were averaged across left and right stimulation sites since we were interested in the general magnitude of changes from functionally similar regions. In support of this data reduction primarily driven by our broad interest in coarse parietal/occipital stimulation differences, follow-on analyses did not show any differences in consistency of network changes between left and right stimulation, using a temporal consensus method inspired by Doron and colleagues (Doron et al., 2012).

Statistical Analyses

To find the substantial changes in metrics across the pre-TMS and post-TMS intervals, traditional linear statistics were used, where the pre-TMS and post-TMS intervals were treated as *conditions* and paired-sample t-tests were applied to node or communities as indicated in the text. In cases where multiple comparisons were carried out (e.g., Figure 5), a Bonferroni correction to the alpha value was used to determine significance. For the correction, each band-specific metric was treated as a separate set of tests (10 comparisons within a set, Community 1 vs Community 2, Community 1 vs Community 3, etc), so the corrected alpha value was set to 0.005. Where appropriate, both the corrected and uncorrected significant comparisons are shown (see Figures 5 and 6).

RESULTS

Here we studied the brain dynamics following single pulses of TMS to occipital and parietal cortex using recently developed approaches from network science. First, we reconstructed estimated neural sources on a volumetric brain mesh and then extracted time series for 68 brain regions (Figure 1). Using a two second epoch surrounding stimulation (-1 to 1), we computed functional connectivity between all

region pairs using the debiased weighted phase lag index (dwPLI) that has shown robustness to noise (Vinck et al., 2011; Vindiola et al., 2014). Our analysis focused on connectivity in the alpha and beta frequency bands since these bands have been suggested as resonant frequencies within the stimulated regions, alpha in occipital and beta in parietal regions (Laufs et al., 2003; Rosanova et al., 2009).

Stimulation Effects on Whole-brain Connectivity

We began by examining patterns of functional connectivity in a whole-brain analysis (see Figure 3). We observed higher connectivity across the brain within the alpha band (8-12Hz) both before (black dotted line in Figure 3A) and after stimulation to either site in bilateral occipital cortex (red line) or bilateral parietal cortex (blue line) compared to other frequency bands. This dominant response in whole-brain alpha synchrony likely reflects its role as a diffuse, communicative signal with multiple functions (Başar et al., 1999), serving as a global signal for sensory and information processing.

We next investigated changes in connectivity following stimulation by comparing changes between pre and post TMS intervals. As shown in Figure 3A, we observed that the average connectivity between region pairs did not show much change within the alpha band after stimulation to either occipital or parietal sites (Occipital: $t(9) = -1.43$, $p = 0.19$; Parietal: $t(9) = -0.72$, $p = 0.49$, all uncorrected), and this was mirrored in the beta band with minimal connectivity differences for both stimulation locations (Occipital: $t(9) = -1.21$, $p = 0.26$; Parietal: $t(9) = -0.52$, $p = 0.61$, all uncorrected). However, there was a marked difference between alpha and beta connectivity when examining the directionality of the change following stimulation (Figure 3B-E). By subtracting the postTMS dwPLI estimate from the preTMS baseline, we observed increased connectivity in the alpha band (Figure 3B-C) for the regional pairs with the largest differences (95th percentile of connections plotted) following stimulation compared to decreases within the beta band (Figure 3D-E). Collectively, these whole-brain connectivity results do not show a strong frequency-specific effect for the stimulation sites, as might have be predicted based on theories that suggest that stimulation could be facilitated or decremented by the inherent resonant

frequency of the tissue (Rosanova et al., 2009). However, this observation could reflect the global influence of these regions on whole-brain connectivity rather than their targeted effects on subnetworks. Consequently, we next employed recent methods from network science to examine the effect of stimulation at a finer scale than average connectivity across nodes.

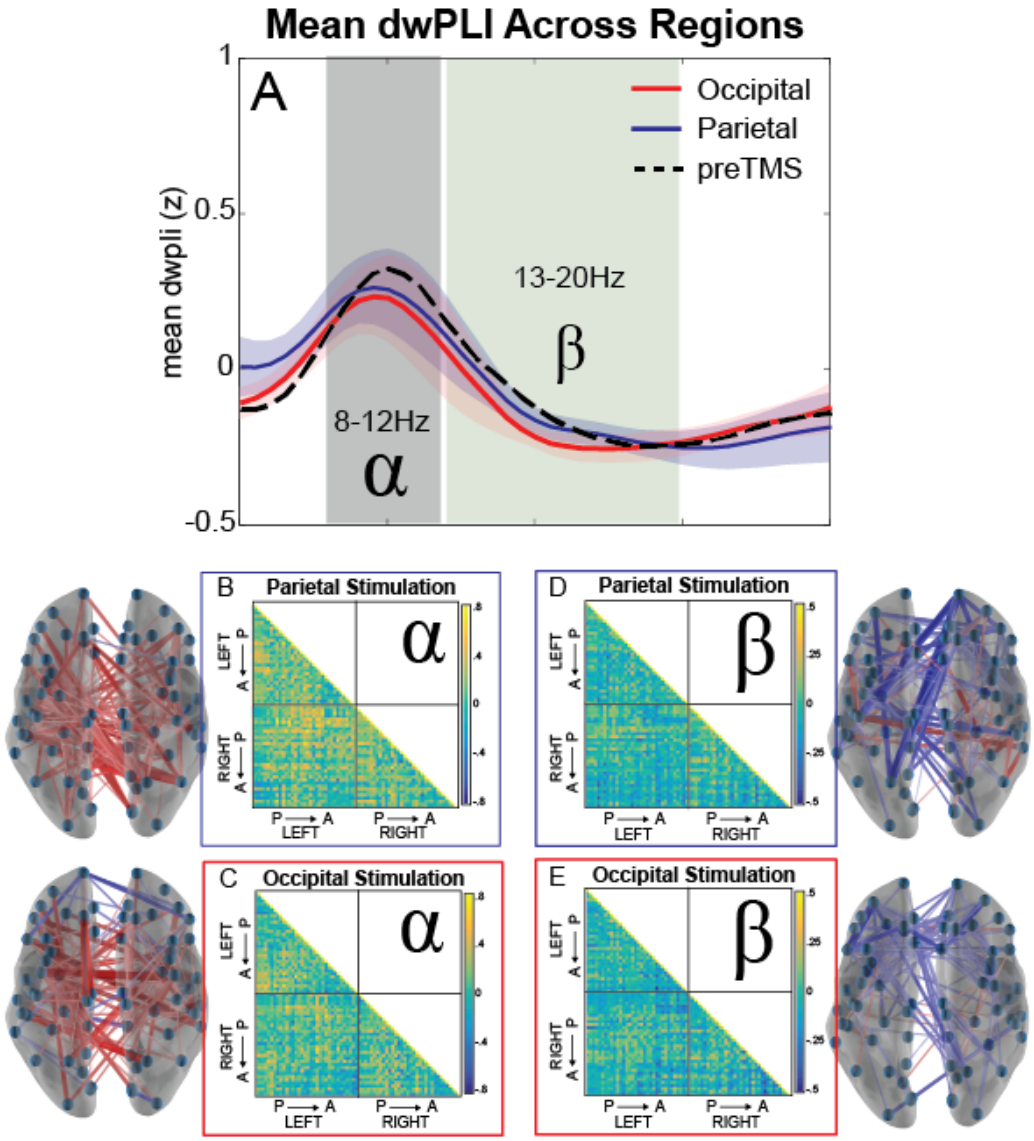

Figure 3: Whole-brain Connectivity Changes Following Stimulation. (A) Average dwPLI across the brain between 5Hz and

25Hz shows higher dwPLI within the alpha band with or without stimulation. (B, C) Debiased weighted phase lag index (dwPLI) differences between the second after TMS (postTMS) and the second before TMS (preTMS) intervals across trials after parietal stimulation (B) and occipital stimulation (C) averaged across the alpha band. (D, E) Results similar to panels B-C but for the beta band. Brain insets display the highest 5% of connections across the brain, providing a topographical illustration of the connectivity matrices where red lines indicate increased connectivity following stimulation and blue lines indicate decreased connectivity following stimulation.

Community Organization in Resting Networks

To examine stimulation effects in brain communities, we capitalized on a network science approach that has been used previously to study modularity in brain networks. To estimate dynamic community structure, we used a Louvain-like greedy algorithm to maximize a multilayer modularity quality function, thereby identifying regions that form modules that would be optimal for cohesive processing (Achard et al., 2006; Sporns et al., 2004). This data-driven approach showed more local granularity in the network landscape following stimulation. Importantly, we defined network communities without stimulation during a period of rest. This allowed us to interrogate the dynamics of community reconfigurations following TMS, given a natural baseline. We defined network communities separately for both the alpha and beta bands, and used the most robust arrangement across the 100 iterations of modularity maximization as the final community structure. The 100 iterations of the preTMS interval were remarkably robust and consistent, showing 100% agreement across iterations for the alpha band and 98% agreement across the iterations within the beta band. We also observed noteworthy similarity (approximately 97% spatial similarity) between them except for a small cluster of motor-related brain regions (Figure 4).

In the alpha band (Fig. 4, *left*), five communities are illustrated: a bilateral occipital-parietal network (Occ, blue), a right paracentral community (RPC, pink), a left temporal network (LTem, yellow), a right temporal network (RTem, green), and a bilateral frontal network (Fron, orange). This largest community (Occ) is a large cluster of regions in occipital and parietal cortex, an organization that is perhaps

unsurprising, given the commonly observed peak of the alpha rhythm within occipital-parietal regions (Hari and Salmelin, 1997). Interestingly, five similar communities were also found within the beta band (Fig. 4 right), and the only observed difference was in the right paracentral community (DKT atlas regions: R precentral, R postcentral). In addition to the two nodes of the pre- and post-central sulcus in the alpha RPC community, the beta band RPC community also contained regions of the medial paracentral lobule, putative sources of motor-related planning (DKT atlas regions: R paracentral, R posterior cingulate). This RPC community in beta nicely aligns with previous literature that implicates the beta band in motor-related activity (Pfurtscheller et al., 1996a), providing support that the detected network communities captured frequency-specific effects.

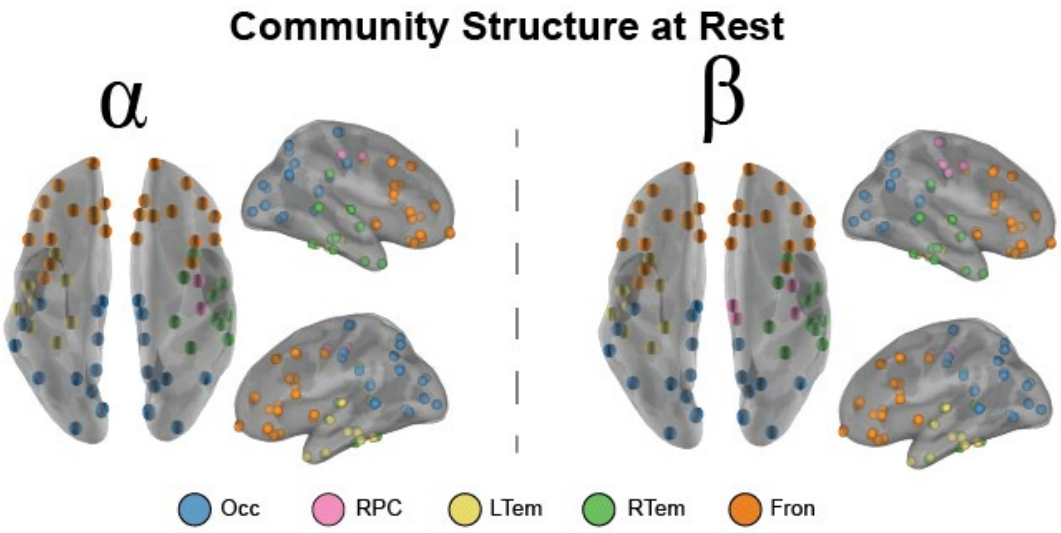

Figure 4: Communities derived from the interregional allegiance matrix in the preTMS interval for the alpha and beta bands. Inflated mesh visualizations of brain regions colored by community organization. Orbs are plotted at the centroid of the regions of interest. Community organization was found independently for the alpha band (Left) and beta band (Right) before stimulation with TMS.

Community Allegiance Differentiates Beta Band Communities from the Alpha Band

We next examined whether stimulation caused dynamic network reconfigurations from the natural baseline resting state. We employed a metric of allegiance that captures how often two nodes are present within the same community before and after stimulation. Figure 5 (A, C) shows the average pair-wise difference in allegiance before and after stimulation within each of the five communities identified from the preTMS resting state connectivity ($Alleg_{post}$-$Alleg_{pre}$). Within the alpha band (top row), we observe clear specificity to the stimulation site when considering changes in the magnitude of allegiance across communities. For occipital stimulation, allegiance change is highest for the occipital-parietal community (Occ) and lowest for the frontal community (Fron; paired t-test, $t(9) = 3.8$, $p = 0.004$, uncorrected). Parietal stimulation does not significantly modulate any community in the alpha band (all $p > 0.05$). The beta band (bottom row), however, shows clear community specificity, where allegiance of the right paracentral (RPC) community is significantly higher than the right temporal (RTem) and frontal (Fron) communities (paired t-tests; RTem, $t(9) = -2.6$, $p = 0.028$; Fron, $t(9) = -2.8$, $p = 0.020$, all uncorrected).

We also examined whether the community allegiance depended on distance from the stimulation site, which we operationalized as the Euclidean distance from the centroid of the community to the node closest to the stimulation site. The effects of stimulation within the alpha band revealed that the nodes closest to the stimulation site are most susceptible to stimulation, and this influence steadily decreased for communities farther from the stimulation site (Figure 5B). This finding suggests that the alpha band is influenced by TMS much like a model of electric field drop-off from the site of stimulation would predict (Thielscher et al., 2015); that is, the stimulation effect decreases as distance from the stimulation site increases. This distance-based effect, however, was not robust, where only 2 of the 10 subjects for parietal stimulation show a significant predictive relationship between the allegiance and Euclidian distance from the stimulation sight to the centroid of each region (136 total regions, 68 regions X 2 hemispheres) using linear regression ($F(2,272) = 4.5$, $p = 0.04$; $F(2,272) = 4.0$, $p = 0.05$).

In contrast, only the RPC community in the beta band was impacted by stimulation (Figure 5D, pink RPC nodes). Thus, for the beta band, stimulation doesn't follow the simple linear model based on distance from the stimulation site as observed in alpha; instead, the stimulation effect is strongest in the RPC community, suggestive of resonant frequencies within the regions targeted (Rosanova et al., 2009). This observation aligns with the *natural frequencies* account of stimulation based on the strong role that beta band serves in motor-related activity (Pfurtscheller et al., 1996a), and the prevalence of motor regions within the RPC community. These results may indicate the importance of pairwise regional activity within a community, so we next examined a network measure of flexibility to investigate regional dynamics.

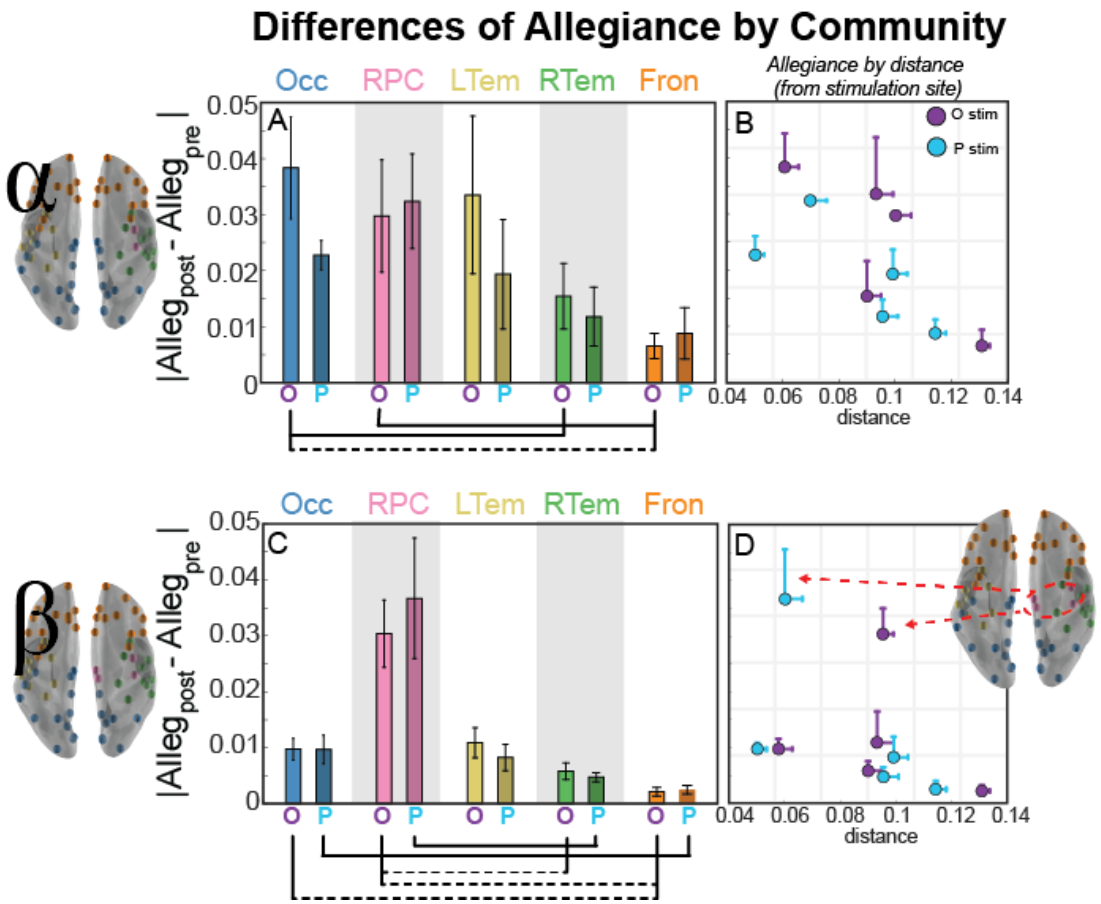

Figure 5: Community allegiance changes within alpha (top) and beta (bottom) band network as a function of distance from the

stimulation site. (A, C) Bar plot of the mean magnitude change (SEM across subjects) from the preTMS interval in pair-wise allegiance from the stimulation site with the bar labeled O for occipital stimulation and P for parietal stimulation. For paired t-test between communities, dotted lines connecting communities indicate uncorrected significance ($p < 0.05$), while solid lines indicate significance corrected for multiple comparisons (Bonferroni, $p < 0.05$). (B,D) Scatter visualization of the mean magnitude allegiance change from the pre-TMS interval shown in (A,C), but now plotted as a function of distance from the stimulation site. Error bars indicate SEM across subjects (allegiance) or nodes within the community (distance) and the color of the marker indicates stimulation site (Occipital in purple and Parietal in blue). Brain inset for the beta band shows the nodes of the RPC community that are most affected by TMS regardless of stimulation site.

Flexibility Differences Indicate Whole-brain Effects within the Alpha Band

As a complement to allegiance, which measures the temporal consistency of community structure at the inter-regional level, we investigated flexibility, a metric that describes how often each node changes the community to which it is allied. This analysis captures whether stimulation drives certain brain regions to cohere with different communities in a manner that is different from their community participation prior to stimulation.

Figure 6 shows the differences in flexibility, averaged across nodes within a community, before and after stimulation ($Flex_{post}$-$Flex_{pre}$). Within the alpha band (top row), we observed minimal difference between communities or stimulation sites; rather, TMS is associated with a statistically equivalent change in flexibility across communities. For the beta band (bottom row), a single community stands out. The RPC community is again the most flexible following TMS. For occipital stimulation, flexibility of the right paracentral (RPC) community is significantly higher than the occipital-parietal (Occ) and trending for right temporal (RTem) communities (paired t-tests; Occ, $t(9) = -3.0$, $p = 0.016$, uncorrected; RTem, $t(9) = -2.2$, $p = 0.057$, uncorrected). This difference is even stronger for parietal stimulation, where flexibility for RPC is tends to be higher than that observed in the left temporal (LTem), right temporal (RTem), frontal (Fron), and significant (Bonferroni corrected) when compared to occipital-parietal (Occ)

communities (paired t-tests; LTem, $t(9) = -3.1$, $p = 0.013$; RTem, $t(9) = -2.6$, $p = 0.030$; Fron, $t(9) = -3.1$, $p = 0.014$; Occ, $t(9) = -4.0$, $p = 0.003$, all uncorrected). These results are reminiscent of the pair-wise allegiance difference showing an increase within a single community (Figure 5C).

We next examined whether flexibility depended on distance from the stimulation site. Alpha communities showed minimal dependence between distance and flexibility (Figure 6B), but there was no significant difference across any of the communities (Figure 6A). In contrast, when we considered flexibility within the beta band, we observed that the RPC community displayed the strongest effect of stimulation (Figure 6D). Combined, these flexibility results demonstrate consistency with the allegiance results, suggesting an effect of resonant frequency in the RPC community for the beta band. However, the communities have variable numbers of nodes and a few nodes could substantially influence the means shown in Figures 5 and 6, so our final analysis examined individual node dynamics to determine whether the smaller size of the RPC community was the primary driver of beta band effects.

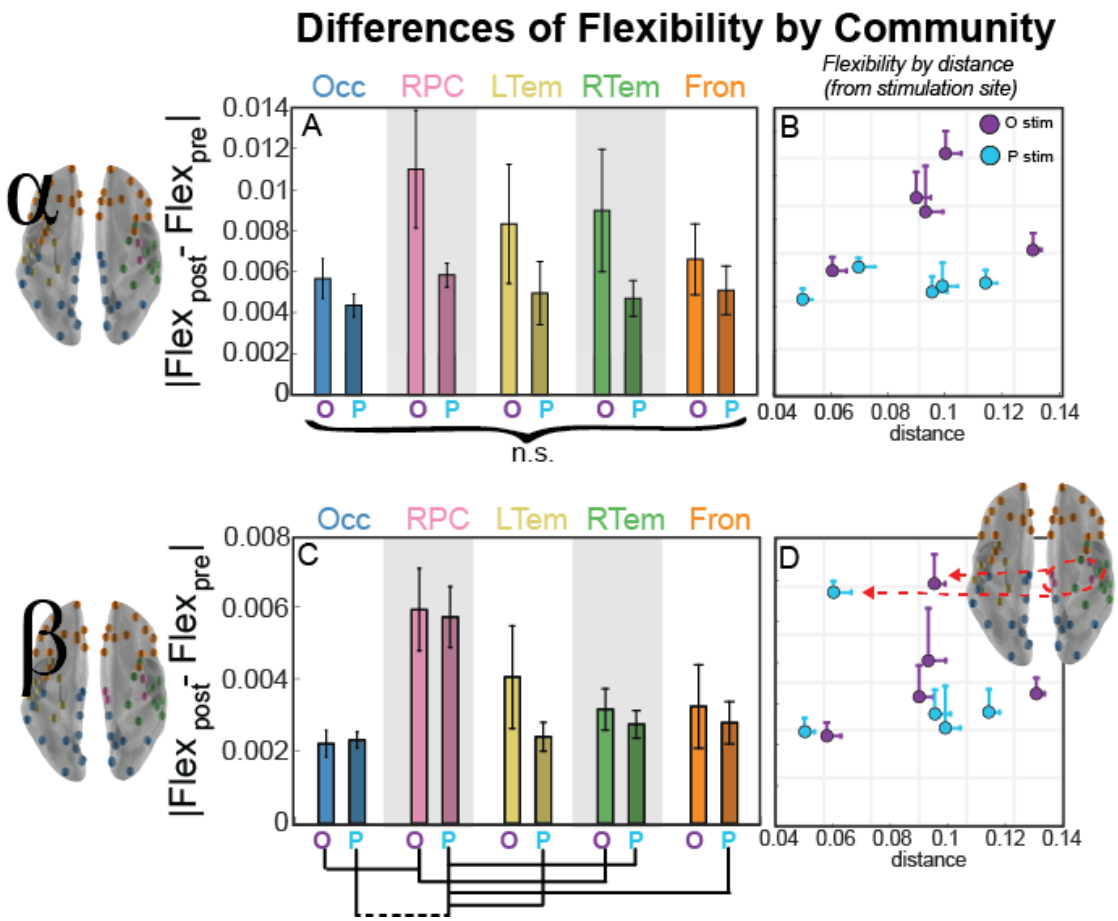

Figure 6: Community flexibility changes within alpha (top) and beta (bottom) band network as a function of distance from the stimulation site. (A, C) Bar plot of the mean magnitude change (SEM across subjects) from the preTMS interval in flexibility as a function of the distance from the stimulation site with the bar labeled O for occipital stimulation and P for parietal stimulation. For paired t-test between communities, dotted lines connecting communities indicate uncorrected significance ($p < 0.05$), while solid lines indicate significance corrected for multiple comparisons (Bonferroni, $p < 0.05$). (B,D) Scatterplot of the mean change in flexibility from the pre-TMS interval shown in (A,C), but now plotted as a function of distance from the stimulation site. Error bars indicate SEM across subjects (flexibility) or nodes within the community (distance) and the color of the marker indicates stimulation site (Occipital in purple and Parietal in blue). Brain inset shows the nodes of the RPC community that are most affected by TMS regardless of stimulation site.

Individual Node Clusters Suggest a Reconfiguration of the Beta Band Network after TMS

Since all of the previous analyses examined only the overall community differences, our final analysis examined the individual node allegiance to the stimulation site and flexibility changes after stimulation. This analysis examines the spatial specificity of the TMS modification of the graph metrics that may be masked by averaging across many nodes within the affiliated community. Figure 7 displays individual node magnitude allegiance (top row) and flexibility (bottom row) differences in the 5 communities of the beta band network following stimulation to occipital (left) and parietal (right) cortex. Overall, there is an increase in allegiance within a narrow range of distances from the stimulation site when considering both occipital (Figure 7A) and parietal stimulation (Figure 7B). Although regions in the right paracentral community (RPC, pink) show increased allegiance, several nodes from other communities also have a similar response profile. To examine the spatial topology of these effects, the brain insets illustrate nodes corresponding to top 15% of allegiance increases (nodes on or above the threshold line in Figure 7A-B). The most influenced nodes surround the sensorimotor regions of the brain, including the RPC community and nearby regions around the central sulcus, the rolandic sites of the brain.

In contrast, the individual node flexibility changes are more diffuse (Figure 7, bottom row). The nodes corresponding to top 15% of flexibility are plotted above the threshold line, and these effects span a larger range of distances than the allegiance changes. However, the spatial topology is quite similar. Flexibility also increases most strongly in a cluster of nodes surrounding the central sulcus. Collectively, these results reveal that the nodes in the RPC community were not uniquely influenced; instead, the network dynamics of the RPC and its surrounding sensorimotor regions show the largest flexibility and allegiance changes within the beta band communities. Together these results show complex network dynamics following stimulation and suggest a *reconfiguration* of the resting beta community organization, rather than a single community enhancement.

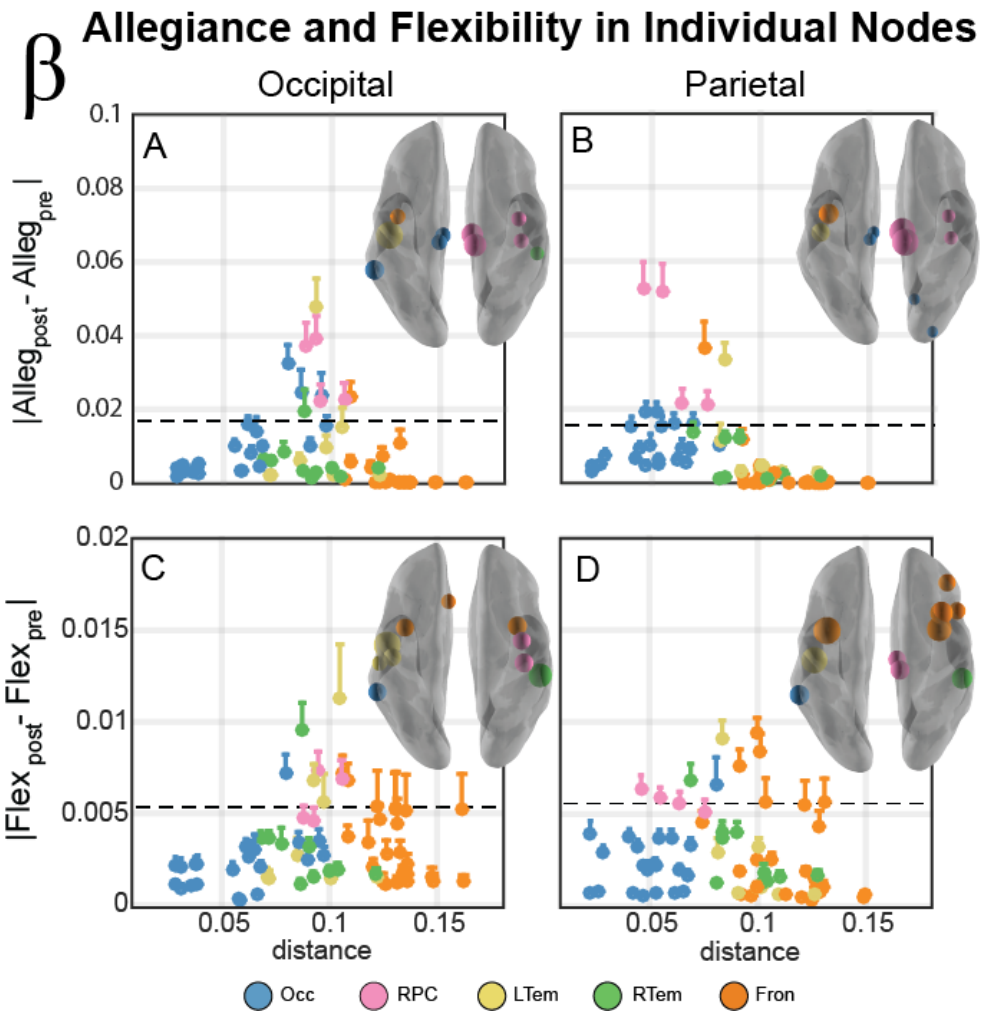

Figure 7: Individual node allegiance (A,B) and flexibility (C,D) changes within the beta band network. (A,B) Individual nodes module allegiance difference ($Alleg_{post}$ – $Alleg_{pre}$) plotted as a function of distance from the stimulation site for occipital (A) and parietal (B) stimulation sites. Color of node describes the community affiliation, and error bars indicate the standard error of the mean. Brain insets display the 85th percentile of module allegiance across all nodes, with nodes scaled by the relative magnitude of this allegiance change. The absolute magnitude of this percentile is also indicated by a horizontal dotted line in each plot. (C,D) Individual nodes flexibility difference ($Flex_{post}$ – $Flex_{pre}$) plotted as a function of distance from the stimulation site for occipital (A) and parietal (B) stimulation sites. Color of nodes, error bars, and brain inset display the same properties as above but in this panel with flexibility rather than allegiance.

DISCUSSION

We investigated network reconfiguration in resting state EEG following single pulses of transcranial magnetic stimulation (TMS) using a method from network science that allows for a quantitative description of the brain's modular architecture (Bassett and Bullmore, 2006; Bullmore and Sporns, 2012; Ercsey-Ravasz et al., 2013). Our analysis focused on connectivity differences between the one second before stimulation and the one second after stimulation. More specifically, we examined network differences in the alpha and beta frequency bands since these bands have been suggested as resonant frequencies within the stimulated regions: alpha in occipital and beta in parietal regions (Laufs et al., 2003; Rosanova et al., 2009).

Our results first examined whole-brain effects of stimulation, and we observed differential effects on connectivity in both alpha and beta activity, although no stark differentiation was seen between stimulation to occipital or parietal sites. Next, we employed a network theoretical approach to identify communities from the resting state EEG data, and we observed several differences in the structure of functional connectivity in both frequency bands after TMS. Within the alpha band, stimulation produced local effects, but interestingly, stimulation also produced more global effects, altering network flexibility across *all* communities when applied to either occipital or parietal cortex. In stark contrast, beta band activity showed high specificity of TMS-induced effects on allegiance and flexibility within a rather focal paracentral network near sensorimotor cortex. These novel results using network science approaches with TMS/EEG revealed an interesting interplay between local and global activity across frequency bands that might underlie how network reconfigurations give rise to coordinated brain activity.

Global effects within the alpha band manifest in similar flexibility across communities

We have shown that TMS to resonating communities constrained within the alpha band has equivalent impact on the overall flexibility of all communities. This finding implies a global impact of stimulation, regardless of stimulation site, to the alpha band networks. Since the first observations of the alpha band by Berger (1929), alpha band activity (8-12Hz), also known as the *Berger rhythm*, has

been a brain rhythm of frequent study due to its dominance in resting EEG, and it is often the only visually observable pattern to the naked eye in the EEG trace. Since its first observation, several hypotheses have been proposed ascribing a functional role to its presence in EEG. The first theory was proposed by Adrian and Mathews (1934) who found that the power within the alpha band increases when subjects are awake with eyes closed. They interpreted this as alpha band activity reflecting a brain-state of inactivity, priming the brain for incoming information. This theory has been expanded and revised to more clearly represent 'cortical idling' (Pfurtscheller et al., 1996b). Recently, however, this theory has been somewhat abandoned because of the difficulty of reconciling it with behavioral experiments that indicate a functional role for power within this band. For example, alpha band activity is also associated with working memory load (Jensen et al., 2002; Klimesch, 1996; Tuladhar et al., 2007). Thus, beyond this 'spontaneous' alpha rhythm, researchers have discovered other forms of alpha, so-called 'functional' alpha (Başar, 2012), which is observed during many cognitive and motor processes. These theories have been further broadened, suggesting alpha activity may even be an *access controller* to a knowledge system (Klimesch, 2012). Collectively, however, alpha activity consistently represents a diffuse, communicative signal with multiple functions, an arguably global signal in terms of its impact on sensory information.

Research using TMS to investigate the functional connectivity within the alpha band, however, provides a more limited view of alpha activity. For example, Rosanova et al. (2009) showed that enhancement of the alpha band is primarily restricted to occipital cortex, regardless of stimulation site. These researchers noted that occipital cortex might *resonate* at the alpha frequency. Our results expand the theory proposed by Rosanova and colleagues by showing that the brain may be parsed into separate resonating communities within the alpha band and each cluster is overall equally modified by TMS, as indicated by the similar flexibility metrics across the resonating communities. Interestingly, however, nodal allegiance to the stimulation site reveals a rather direct and localized impact within the occipital and parietal cortex: specifically the cluster that is most associated with alpha band activity. Together,

these results suggest a process whereby alpha connectivity can provide both the specific visual effects shown in early studies while also serving many functional roles across disparate brain regions.

Local effects of beta band manifest in the specificity of network changes within the paracentral community

Two pieces of evidence in the current study converge to show that the paracentral network plays a highly specific role in dynamic network reconfiguration within the beta band, and our results support and extend the natural frequency theory of the brain following single pulses of TMS (Rosanova et al., 2009). First, the network communities defined on resting state activity are identical between alpha and beta bands, except for the right paracentral network (RPC). The beta-band RPC consists of nodes within the paracentral lobule and two nodes within the pre and post central gyri that have been in sensorimotor processing, and previous research has consistently identified motor-related activity in the beta band (Pfurtscheller et al., 1996b). Second, following a single TMS pulse to either stimulation site, we observe that the paracentral region uniquely displays both the highest flexibility and allegiance changes from the baseline state in the beta band, but not the alpha band. Together, these findings suggest a unique specificity that would support the natural frequency theory of TMS. In fact, our results provide intuition at a level of granularity that has not been previously explored, by capitalizing on recently developed methods from network science (Bassett and Sporns, 2017) to investigate perturbations of brain networks following single pulses of TMS.

The granularity of this effect was further enhanced by inspection of the nodal allegiance and flexibility across the brain. The RPC community was clearly involved and appeared to be an isolated community with increased nodal allegiance (among its nodes) and global flexibility in the beta-band communities. However, when we inspected the single nodes contributing to this effect, we found that this effect was not constrained by the boundaries of the beta-band RPC network as we defined from baseline activity. Instead, the effects spread to nodes outside this RPC community and consisted of a

cluster of nodes surrounding the central sulcus. This granularity of the beta band network effects after TMS aligns well with the well-known involvement of rolandic sites in sensorimotor processes and discharges of beta-band activity (Baker, 2007).

Clinical Implications

TMS has been used successfully in clinical settings for treating movement disorders (Pascual-Leone et al., 1994) and mitigating severe affective disorders (Berman et al., 2000); however, some studies that have investigated the efficacy and efficiency of TMS treatment for depression (for review, Loo & Mitchell, 2005) suggest that most treatment regimens are suboptimal, often stimulating for a duration of two weeks and only having a minor benefit. Here we have shown a complex interplay between local and global neural processing, but more generally, our results speak to the specificity of TMS, where particular resonating communities of brain regions (e.g., beta band activity emanating from sensorimotor regions) or diffuse sets of resonating communities (e.g., all regions in alpha band) may be modified by TMS regardless of stimulation site. In other words, we show that stimulating a focal region can have distal effects on many other brain regions. Future studies expanding on how individual variability in brain connectivity impacts how TMS propagates through cortex may eventually reveal the specific networks or brain regions that may predict successful treatment. We believe the methods and initial results within this work hold promise in future studies to help determine stimulation protocols for a variety of clinical settings and surrounding several cognitive domains.

Our results first examined whole-brain effects of stimulation, and we observed differential effects on connectivity in both alpha and beta activity, although no stark differentiation was seen between stimulation to occipital or parietal sites. Next, we employed a network theoretical approach to identify communities from the resting state EEG data, and we observed several differences in the structure of functional connectivity in both frequency bands after TMS. Within the alpha band, stimulation produced local effects, but interestingly, stimulation also produced more global effects, altering network flexibility

across *all* communities when applied to either occipital or parietal cortex.

Methodological considerations

Our use of community detection to understand functional connectivity in the brain and the effects of TMS on specific brain networks focuses on two stimulation sites and two common frequency bands. We use a phase-based undirected connectivity measurement and inspect graph metric changes at a single snapshot of the available parameters within the dynamic modularity framework we applied. This initial implementation of a graph theoretical approach on human neurostimulation effects may be expanded in the future to investigate the directed communication between these resonating communities (e.g., Reimann et al., 2017), cross-frequency communication (Canolty and Knight, 2010), and increased resolution across frequencies of the brain.

Our experimental design did not employ neuronavigation or a traditional control stimulation site; instead, our participants completed 4 experimental sessions across 4 different days to maximize the variability in the pre-stim period to identify stimulation effects robust to state differences (boredom, fatigue, mindwandering, etc). However, an interesting avenue for future work would be to examine network changes that may be more closely tied to functionally-localized regions, where neuronavigation would serve a critical role in equating more precise stimulation locations between individuals. Similarly, our analysis did not require a control site since our analysis focused on changes between baseline activity and activity following stimulation. The analytic logic follows the classic subtraction logic between conditions in traditional neuroimaging analysis: conditions are designed to only manipulate the factor of interest, so looking at their difference eliminates all of the concomitant neural processing that occurs but is tangential to condition comparison of interest. Here, the analysis examined differences between occipital and parietal stimulation, so each served as the other’s control for general stimulation effects. However, future research may use more regions and intensities to augment our understanding about differences in ongoing activity with more functionally-determined stimulation protocols.

CONCLUSION

Using a recently developed network-based methodology applied to EEG, we have investigated the reconfigurations of naturally resonating communities of brain regions. While the alpha network reveals the dynamic interplay of local and global activity, communities within the beta band revealed a remarkable specificity, displaying more local connectivity changes. Particularly important next steps include linking these observations with emerging theories of the impact of stimulation on distributed networks in the form of network control theory (Gu et al., 2015), which has begun to offer insights into the brain's preference for certain low energy states (Betzel et al., 2017), the role that brain topology plays on the energy requires for brain state transitions (Kim et al., in press; Tang and Bassett, in press), and the predicted impact of stimulation on distal areas (Gu et al., in press; Muldoon et al., 2016). Efforts to ground TMS studies like the one we report here in a mechanistic theory could have lasting consequences in studies linking behavioral changes to neural oscillations or neurostimulation (Medaglia et al., in press), but may also impact future protocols for clinical purposes, providing a means to reconfigure resonating clusters in the brain.

Acknowledgments

The authors acknowledge thoughtful discussions with our colleagues at University of California, Irvine for study coordination and subject testing. This research was supported by mission funding to the U.S. Army Research Laboratory as well as sponsored by the Army Research Laboratory and accomplished under Cooperative Agreement Number W911NF-10-2-0022. We would also like to acknowledge that the work was partially collected while JOG was funded by a National Research Service Award (F31-EY-019241) awarded by NIH. The authors have indicated no financial or non-financial conflicts of interest. The views and conclusions contained in this document are those of the authors and should not be interpreted as representing the official policies, either expressed or implied, of the Army Research Laboratory or the U.S. Government. The U.S. Government is authorized to reproduce and distribute reprints for Government purposes notwithstanding any copyright notation herein.

REFERENCES

Achard, S., Salvador, R., Whitcher, B., Suckling, J., and Bullmore, E. (2006). A Resilient, Low-Frequency, Small-World Human Brain Functional Network with Highly Connected Association Cortical Hubs. J. Neurosci. *26*, 63–72.

Adrian, E.D., and Matthews, B.H.C. (1934). The interpretation of potential waves in the cortex. J. Physiol. *81*, 440–471.

Alivisatos, A.P., Chun, M., Church, G.M., Greenspan, R.J., Roukes, M.L., and Yuste, R. (2012). The Brain Activity Map Project and the Challenge of Functional Connectomics. Neuron *74*, 970–974.

Auriat, A.M., Neva, J.L., Peters, S., Ferris, J.K., and Boyd, L.A. (2015). A Review of Transcranial Magnetic Stimulation and Multimodal Neuroimaging to Characterize Post-Stroke Neuroplasticity. Front. Neurol. *6*.

Azevedo, F.A.C., Carvalho, L.R.B., Grinberg, L.T., Farfel, J.M., Ferretti, R.E.L., Leite, R.E.P., Filho, W.J., Lent, R., and Herculano-Houzel, S. (2009). Equal numbers of neuronal and nonneuronal cells make the human brain an isometrically scaled-up primate brain. J. Comp. Neurol. *513*, 532–541.

Baker, S.N. (2007). Oscillatory interactions between sensorimotor cortex and the periphery. Curr. Opin. Neurobiol. *17*, 649–655.

Başar, E. (2012). A review of alpha activity in integrative brain function: Fundamental physiology, sensory coding, cognition and pathology. Int. J. Psychophysiol. *86*, 1–24.

Başar, E., Başar-Eroğlu, C., Karakaş, S., and Schürmann, M. (1999). Are cognitive processes manifested in event-related gamma, alpha, theta and delta oscillations in the EEG? Neurosci. Lett. *259*, 165–168.

Bassett, D.S., and Bullmore, E. (2006). Small-world brain networks. Neurosci. Rev. J. Bringing Neurobiol. Neurol. Psychiatry *12*, 512–523.

Bassett, D.S., and Sporns, O. (2017). Network neuroscience. Nat. Neurosci. *20*, 353–364.

Bassett, D.S., Wymbs, N.F., Porter, M.A., Mucha, P.J., Carlson, J.M., and Grafton, S.T. (2011). Dynamic reconfiguration of human brain networks during learning. Proc. Natl. Acad. Sci. *108*, 7641–7646.

Bassett, D.S., Wymbs, N.F., Rombach, M.P., Porter, M.A., Mucha, P.J., and Grafton, S.T. (2013). Task-Based Core-Periphery Organization of Human Brain Dynamics. PLoS Comput Biol *9*, e1003171.

Bassett, D.S., Yang, M., Wymbs, N.F., and Grafton, S.T. (2015). Learning-induced autonomy of sensorimotor systems. Nat. Neurosci. *18*, 744–751.

Berger, H. (1929). Electroencephalogram in humans. Arch. Psychiatr. Nervenkr. *87*, 527–570.

Bergmann, T.O., Karabanov, A., Hartwigsen, G., Thielscher, A., and Siebner, H.R. (2016). Combining

non-invasive transcranial brain stimulation with neuroimaging and electrophysiology: Current approaches and future perspectives. NeuroImage *140*, 4–19.

Berman, R.M., Narasimhan, M., Sanacora, G., Miano, A.P., Hoffman, R.E., Hu, X.S., Charney, D.S., and Boutros, N.N. (2000). A randomized clinical trial of repetitive transcranial magnetic stimulation in the treatment of major depression. Biol. Psychiatry *47*, 332–337.

Bestmann, S., Ruff, C.C., Blankenburg, F., Weiskopf, N., Driver, J., and Rothwell, J.C. (2008). Mapping causal interregional influences with concurrent TMS–fMRI. Exp. Brain Res. *191*, 383.

Betzel, R.F., Satterthwaite, T.D., Gold, J.I., and Bassett, D.S. (2017). Positive affect, surprise, and fatigue are correlates of network flexibility. Sci. Rep. *7*, 520.

Bigdely-Shamlo, N., Mullen, T., Kothe, C., Su, K.-M., and Robbins, K.A. (2015). The PREP pipeline: standardized preprocessing for large-scale EEG analysis. Front. Neuroinformatics *9*, 16.

Blondel, V.D., Guillaume, J.-L., Lambiotte, R., and Lefebvre, E. (2008). Fast unfolding of communities in large networks. J. Stat. Mech. Theory Exp. *2008*, P10008.

Bohning, D., Shastri, A., McConnell, K., Nahas, Z., Lorberbaum, J., Roberts, D., Teneback, C., Vincent, D., and George, M. (1999). A combined TMS/fMRI study of intensity-dependent TMS over motor cortex. Biol. Psychiatry *45*, 385–394.

Bortoletto, M., Veniero, D., Thut, G., and Miniussi, C. (2015). The contribution of TMS–EEG coregistration in the exploration of the human cortical connectome. Neurosci. Biobehav. Rev. *49*, 114–124.

Bressler, S.L., and Kelso, J.A.S. (2001). Cortical coordination dynamics and cognition. Trends Cogn. Sci. *5*, 26–36.

Bressler, S.L., and Menon, V. (2010). Large-scale brain networks in cognition: emerging methods and principles. Trends Cogn. Sci. *14*, 277–290.

Brunel, N., and Wang, X.-J. (2003). What Determines the Frequency of Fast Network Oscillations With Irregular Neural Discharges? I. Synaptic Dynamics and Excitation-Inhibition Balance. J. Neurophysiol. *90*, 415–430.

Brunoni, A.R., and Vanderhasselt, M.-A. (2014). Working memory improvement with non-invasive brain stimulation of the dorsolateral prefrontal cortex: A systematic review and meta-analysis. Brain Cogn. *86*, 1–9.

Bullmore, E., and Sporns, O. (2012). The economy of brain network organization. Nat. Rev. Neurosci. *13*, 336–349.

Buzsaki, G. (2006). Rhythms of the Brain (Oxford University Press).

Buzsáki, G., and Draguhn, A. (2004). Neuronal Oscillations in Cortical Networks. Science *304*, 1926–1929.

Buzsáki, G., and Wang, X.-J. (2012). Mechanisms of Gamma Oscillations. Annu. Rev. Neurosci. *35*, 203–225.

Canolty, R.T., and Knight, R.T. (2010). The functional role of cross-frequency coupling. Trends Cogn. Sci. *14*, 506–515.

Cocchi, L., Sale, M.V., Lord, A., Zalesky, A., Breakspear, M., and Mattingley, J.B. (2015). Dissociable effects of local inhibitory and excitatory theta-burst stimulation on large-scale brain dynamics. J. Neurophysiol. *113*, 3375–3385.

Cocchi, L., Gollo, L.L., Zalesky, A., and Breakspear, M. (2017). Criticality in the brain: A synthesis of neurobiology, models and cognition. Prog. Neurobiol.

Desikan, R.S., Ségonne, F., Fischl, B., Quinn, B.T., Dickerson, B.C., Blacker, D., Buckner, R.L., Dale, A.M., Maguire, R.P., Hyman, B.T., et al. (2006). An automated labeling system for subdividing the human cerebral cortex on MRI scans into gyral based regions of interest. NeuroImage *31*, 968–980.

van Diessen, E., Numan, T., van Dellen, E., van der Kooi, A.W., Boersma, M., Hofman, D., van Lutterveld, R., van Dijk, B.W., van Straaten, E.C.W., Hillebrand, A., et al. (2015). Opportunities and methodological challenges in EEG and MEG resting state functional brain network research. Clin. Neurophysiol. *126*, 1468–1481.

Doron, K.W., Bassett, D.S., and Gazzaniga, M.S. (2012). Dynamic network structure of interhemispheric coordination. Proc. Natl. Acad. Sci. *109*, 18661–18668.

Driver, J., Blankenburg, F., Bestmann, S., Vanduffel, W., and Ruff, C.C. (2009). Concurrent brain-stimulation and neuroimaging for studies of cognition. Trends Cogn. Sci. *13*, 319–327.

Eldaief, M.C., Press, D.Z., and Pascual-Leone, A. (2013). Transcranial magnetic stimulation in neurology. Neurol. Clin. Pract. *3*, 519–526.

Ercsey-Ravasz, M., Markov, N.T., Lamy, C., Van Essen, D.C., Knoblauch, K., Toroczkai, Z., and Kennedy, H. (2013). A Predictive Network Model of Cerebral Cortical Connectivity Based on a Distance Rule. Neuron *80*, 184–197.

Evans, A.C., Collins, D.L., Mills, S.R., Brown, E.D., Kelly, R.L., and Peters, T.M. (1993). 3D statistical neuroanatomical models from 305 MRI volumes. In Nuclear Science Symposium and Medical Imaging Conference, 1993., 1993 IEEE Conference Record., pp. 1813–1817 vol.3.

Fries, P., Nikolić, D., and Singer, W. (2007). The gamma cycle. Trends Neurosci. *30*, 309–316.

Garcia, J.O., Grossman, E.D., and Srinivasan, R. (2011). Evoked potentials in large-scale cortical networks elicited by TMS of the visual cortex. J. Neurophysiol. *106*, 1734–1746.

Garcia, J.O., Ashourvan, A., Muldoon, S., Vettel, J.M., and Bassett, D.S. (2018). Applications of Community Detection Techniques to Brain Graphs: Algorithmic Considerations and Implications for Neural Function. Proc. IEEE *106*, 846–867.

Geisler, C., Brunel, N., and Wang, X.-J. (2005). Contributions of intrinsic membrane dynamics to fast network oscillations with irregular neuronal discharges. J. Neurophysiol. *94*, 4344–4361.

Gollo, L.L., Roberts, J.A., and Cocchi, L. (2017). Mapping how local perturbations influence systems-level brain dynamics. NeuroImage.

Good, B.H., de Montjoye, Y.-A., and Clauset, A. (2010). Performance of modularity maximization in practical contexts. Phys. Rev. E *81*, 046106.

Gramfort, A., Papadopoulo, T., Olivi, E., and Clerc, M. (2010). OpenMEEG: opensource software for quasistatic bioelectromagnetics. Biomed. Eng. OnLine *9*, 45.

Gu, S., Cieslak, M., Baird, B., Muldoon, S.F., Grafton, S.T., Pasqualetti, F., and Bassett, D.S. (in press). The energy landscape of neurophysiological activity implicit in brain network structure. NeuroImage.

Gu, S., Pasqualetti, F., Cieslak, M., Telesford, Q.K., Yu, A.B., Kahn, A.E., Medaglia, J.D., Vettel, J.M., Miller, M.B., Grafton, S.T., et al. (2015). Controllability of structural brain networks. Nat. Commun. *6*, ncomms9414.

Hari, R., and Salmelin, R. (1997). Human cortical oscillations: a neuromagnetic view through the skull. Trends Neurosci. *20*, 44–49.

Herring, J.D., Thut, G., Jensen, O., and Bergmann, T.O. (2015). Attention Modulates TMS-Locked Alpha Oscillations in the Visual Cortex. J. Neurosci. *35*, 14435–14447.

Hillebrand, A., Barnes, G.R., Bosboom, J.L., Berendse, H.W., and Stam, C.J. (2012). Frequency-dependent functional connectivity within resting-state networks: An atlas-based MEG beamformer solution. NeuroImage *59*, 3909–3921.

Holmes, C.J., Hoge, R., Collins, L., Woods, R., Toga, A.W., and Evans, A.C. (1998). Enhancement of MR images using registration for signal averaging. J. Comput. Assist. Tomogr. *22*, 324–333.

Jensen, O., Gelfand, J., Kounios, J., and Lisman, J.E. (2002). Oscillations in the alpha band (9-12 Hz) increase with memory load during retention in a short-term memory task. Cereb. Cortex N. Y. N 1991 *12*, 877–882.

Kim, J., Soffer, J.M., Kahn, A.E., Vettel, J.M., Pasqualetti, F., and Bassett, D.S. (in press). Topological Principles of Control in Dynamical Network Systems. Nat. Phys.

Klimesch, W. (1996). Memory processes, brain oscillations and EEG synchronization. Int. J. Psychophysiol. *24*, 61–100.

Klimesch, W. (2012). Alpha-band oscillations, attention, and controlled access to stored information. Trends Cogn. Sci. *16*, 606–617.

Kothe, C.A., and Makeig, S. (2013). BCILAB: a platform for brain-computer interface development. J. Neural Eng. *10*, 056014.

Kybic, J., Clerc, M., Abboud, T., Faugeras, O., Keriven, R., and Papadopoulo, T. (2005). A common formalism for the Integral formulations of the forward EEG problem. IEEE Trans. Med. Imaging *24*, 12–28.

Mancini, M., Mastropasqua, C., Bonnì, S., Ponzo, V., Cercignani, M., Conforto, S., Koch, G., and Bozzali, M. (2017). Theta Burst Stimulation of the Precuneus Modulates Resting State Connectivity in the Left Temporal Pole. Brain Topogr. *30*, 312–319.

Massimini, M., Tononi, G., and Huber, R. (2009). Slow waves, synaptic plasticity and information processing: insights from transcranial magnetic stimulation and high-density EEG experiments. Eur. J. Neurosci. *29*, 1761–1770.

Medaglia, J.D., Huang, W., Karuza, E.A., Thompson-Schill, S.L., Ribeiro, A., and Bassett, D.S. (in press). Functional Alignment with Anatomical Networks is Associated with Cognitive Flexibility. Nat. Hum. Behav.

Mucha, P.J., Richardson, T., Macon, K., Porter, M.A., and Onnela, J.P. (2010). Community structure in time-dependent, multiscale, and multiplex networks. Science *328*, 876–878.

Muldoon, S.F., Pasqualetti, F., Gu, S., Cieslak, M., Grafton, S.T., Vettel, J.M., and Bassett, D.S. (2016). Stimulation-Based Control of Dynamic Brain Networks. PLOS Comput. Biol. *12*, e1005076.

Mullen, T.R. (2014). The Dynamic Brain: Modeling Neural Dynamics and Interactions From Human Electrophysiological Recordings. UNIVERSITY OF CALIFORNIA, SAN DIEGO.

Mullen, T.R., Kothe, C.A.E., Chi, Y.M., Ojeda, A., Kerth, T., Makeig, S., Jung, T.-P., and Cauwenberghs, G. (2015). Real-time neuroimaging and cognitive monitoring using wearable dry EEG. IEEE Trans. Biomed. Eng. *62*, 2553–2567.

Nunez, P.L., and Srinivasan, R. (2006). Electric Fields of the Brain: The Neurophysics of EEG (Oxford University Press).

Nunez, P.L., Wingeier, B.M., and Silberstein, R.B. (2001). Spatial-temporal structures of human alpha rhythms: Theory, microcurrent sources, multiscale measurements, and global binding of local networks. Hum. Brain Mapp. *13*, 125–164.

Oostenveld, R., Fries, P., Maris, E., and Schoffelen, J.-M. (2010). FieldTrip: Open Source Software for Advanced Analysis of MEG, EEG, and Invasive Electrophysiological Data. Comput. Intell. Neurosci. *2011*, e156869.

Pascual-Leone, A., Valls-Solé, J., Brasil-Neto, J.P., Cammarota, A., Grafman, J., and Hallett, M. (1994). Akinesia in Parkinson's disease. II. Effects of subthreshold repetitive transcranial motor cortex stimulation. Neurology *44*, 892–898.

Pascual-Leone, A., Walsh, V., and Rothwell, J. (2000). Transcranial magnetic stimulation in cognitive neuroscience – virtual lesion, chronometry, and functional connectivity. Curr. Opin. Neurobiol. *10*, 232–237.

Paus, T. (1998). Imaging the brain before, during, and after transcranial magnetic stimulation. Neuropsychologia *37*, 219–224.

Pfurtscheller, G., Stancák Jr., A., and Neuper, C. (1996a). Post-movement beta synchronization. A correlate of an idling motor area? Electroencephalogr. Clin. Neurophysiol. *98*, 281–293.

Pfurtscheller, G., Stancák, A., and Neuper, C. (1996b). Event-related synchronization (ERS) in the alpha band--an electrophysiological correlate of cortical idling: a review. Int. J. Psychophysiol. Off. J. Int. Organ. Psychophysiol. *24*, 39–46.

Reimann, M.W., Nolte, M., Scolamiero, M., Turner, K., Perin, R., Chindemi, G., Dłotko, P., Levi, R.,

Hess, K., and Markram, H. (2017). Cliques of Neurons Bound into Cavities Provide a Missing Link between Structure and Function. Front. Comput. Neurosci. *11*.

Romei, V., Thut, G., Mok, R.M., Schyns, P.G., and Driver, J. (2012). Causal implication by rhythmic transcranial magnetic stimulation of alpha frequency in feature-based local vs. global attention. Eur. J. Neurosci. *35*, 968–974.

Romei, V., Murray, M.M., Cappe, C., and Thut, G. (2013). The Contributions of Sensory Dominance and Attentional Bias to Cross-modal Enhancement of Visual Cortex Excitability. J. Cogn. Neurosci. *25*, 1122–1135.

Rosanova, M., Casali, A., Bellina, V., Resta, F., Mariotti, M., and Massimini, M. (2009). Natural frequencies of human corticothalamic circuits. J. Neurosci. Off. J. Soc. Neurosci. *29*, 7679–7685.

Rose, N.S., LaRocque, J.J., Riggall, A.C., Gosseries, O., Starrett, M.J., Meyering, E.E., and Postle, B.R. (2016). Reactivation of latent working memories with transcranial magnetic stimulation. Science *354*, 1136–1139.

Rossi, S., Hallett, M., Rossini, P.M., and Pascual-Leone, A. (2009). Safety, ethical considerations, and application guidelines for the use of transcranial magnetic stimulation in clinical practice and research. Clin. Neurophysiol. *120*, 2008–2039.

Sale, M.V., Mattingley, J.B., Zalesky, A., and Cocchi, L. (2015). Imaging human brain networks to improve the clinical efficacy of non-invasive brain stimulation. Neurosci. Biobehav. Rev. *57*, 187–198.

Siebner, H.R., Bergmann, T.O., Bestmann, S., Massimini, M., Johansen-Berg, H., Mochizuki, H., Bohning, D.E., Boorman, E.D., Groppa, S., Miniussi, C., et al. (2009). Consensus paper: Combining transcranial stimulation with neuroimaging. Brain Stimulat. *2*, 58–80.

Sporns, O., Chialvo, D.R., Kaiser, M., and Hilgetag, C.C. (2004). Organization, development and function of complex brain networks. Trends Cogn Sci *8*, 418–425.

Tadel, F., Baillet, S., Mosher, J.C., Pantazis, D., Leahy, R.M., Tadel, F., Baillet, S., Mosher, J.C., Pantazis, D., and Leahy, R.M. (2011). Brainstorm: A User-Friendly Application for MEG/EEG Analysis, Brainstorm: A User-Friendly Application for MEG/EEG Analysis. Comput. Intell. Neurosci. Comput. Intell. Neurosci. *2011*, *2011*, e879716.

Tang, E., and Bassett, D.S. (in press). Control of dynamics in brain networks. Nat. Commun.

Taylor, P.C.J., and Thut, G. (2012). Brain activity underlying visual perception and attention as inferred from TMS–EEG: A review. Brain Stimulat. *5*, 124–129.

Thielscher, A., Antunes, A., and Saturnino, G.B. (2015). Field modeling for transcranial magnetic stimulation: A useful tool to understand the physiological effects of TMS? In 2015 37th Annual International Conference of the IEEE Engineering in Medicine and Biology Society (EMBC), pp. 222–225.

Tuladhar, A.M., ter Huurne, N., Schoffelen, J.-M., Maris, E., Oostenveld, R., and Jensen, O. (2007). Parieto-occipital sources account for the increase in alpha activity with working memory load. Hum. Brain Mapp. *28*, 785–792.

Vinck, M., Oostenveld, R., van Wingerden, M., Battaglia, F., and Pennartz, C.M.A. (2011). An improved index of phase-synchronization for electrophysiological data in the presence of volume-conduction, noise and sample-size bias. Neuroimage *55*, 1548–1565.

Vindiola, M.M., Vettel, J.M., Gordon, S.M., Franaszczuk, P.J., and McDowell, K. (2014). Applying EEG phase synchronization measures to non-linearly coupled neural mass models. J. Neurosci. Methods *226*, 1–14.

Volberg, G., Kliegl, K., Hanslmayr, S., and Greenlee, M.W. (2009). EEG alpha oscillations in the preparation for global and local processing predict behavioral performance. Hum. Brain Mapp. *30*, 2173–2183.